Publications

7-2009

A Near-Infrared Spectroscopic Survey of Cool White Dwarfs in the Sloan Digital Sky Survey

Mukremin Kilic
Smithsonian Astrophysical Observatory

Piotr M. Kowalski
Lehrstuhl fur Theoretische Chemie

Ted von Hippel
Embry-Riddle Aeronautical University, vonhippt@erau.edu

Follow this and additional works at: https://commons.erau.edu/publication

Part of the Stars, Interstellar Medium and the Galaxy Commons

A NEAR-INFRARED SPECTROSCOPIC SURVEY OF COOL WHITE DWARFS IN THE SLOAN DIGITAL SKY SURVEY[*]

MUKREMIN KILIC[1,4], PIOTR M. KOWALSKI[2], AND TED VON HIPPEL[3]
[1] Smithsonian Astrophysical Observatory, 60 Garden Street, Cambridge, MA 02138, USA; mkilic@cfa.harvard.edu
[2] Lehrstuhl für Theoretische Chemie, Ruhr-Universität Bochum, 44780 Bochum, Germany
[3] Physics Department, Siena College, 515 Loudon Road, Loudonville, NY 12211, USA

ABSTRACT

We present near-infrared photometric observations of 15 and spectroscopic observations of 38 cool white dwarfs (WDs). This is the largest near-infrared spectroscopic survey of cool WDs to date. Combining the Sloan Digital Sky Survey photometry and our near-infrared data, we perform a detailed model atmosphere analysis. The spectral energy distributions of our objects are explained fairly well by model atmospheres with temperatures ranging from 6300 K down to 4200 K. Two WDs show significant absorption in the infrared, and are best explained with mixed H/He atmosphere models. Based on the up-to-date model atmosphere calculations by Kowalski & Saumon, we find that the majority of the stars in our sample have hydrogen-rich atmospheres. We do not find any pure helium atmosphere WDs below 5000 K, and we find a trend of increasing hydrogen to helium ratio with decreasing temperature. These findings present an important challenge to understanding the spectral evolution of WDs.

Key words: stars: atmospheres – stars: evolution – white dwarfs

Online-only material: color figures

1. INTRODUCTION

Recent large ground-based surveys, e.g., the Sloan Digital Sky Survey (SDSS), and the space-based surveys of globular clusters are now finding the coolest and oldest white dwarfs (WDs) in the Galactic disk (Gates et al. 2004; Harris et al. 2008) and halo (Hansen et al. 2007). The SDSS spectroscopy uncovered around 10,000 WDs warmer than 7000 K in the Data Release 4 area (Eisenstein et al. 2006). Kilic et al. (2006c) extended the SDSS WD sample to cool WDs by follow-up spectroscopy of high proper motion targets selected using USNO-B and SDSS astrometry (Munn et al. 2004). This enabled Harris et al. (2006) to create a new luminosity function including 6000 WDs. A detailed model atmosphere analysis of these stars is required in order to constrain the faint end of this luminosity function and to make it useful for a precise age determination.

Cool hydrogen-rich WD atmospheres suffer from collision-induced absorption (CIA) due to molecular hydrogen in the infrared (Hansen 1998; Saumon & Jacobson 1999) and Lyα opacity in the ultraviolet (Kowalski & Saumon 2006; Koester & Wolff 2000). The primary opacity source in pure He atmosphere WDs is He$^-$ free–free absorption, and the SEDs of these stars are similar to those of blackbodies (Kowalski et al. 2007). Hence, differentiating between hydrogen- and helium-rich atmosphere solutions and therefore determining the temperatures and bolometric luminosities of cool WDs require a detailed analysis of their optical and infrared spectral energy distributions (SEDs).

Bergeron et al. (1997, 2001) found that most cool WDs have either pure H (DA spectral type) or pure He atmospheres. They also found that the non-DA to DA ratio increases for WDs cooler than 12000 K, but the non-DAs almost disappear in the range 5000–6000 K, and re-appear below 5000 K (the so-called non-DA gap). Bergeron et al. (2001) suggested that an unidentified physical mechanism turns helium-rich WDs into hydrogen-dominated atmospheres at 6000 K, and convective mixing turns some DAs back to helium-dominated atmospheres at 5000 K. Hansen (1999) proposed an alternative solution involving the difference in cooling timescales between DA and non-DA WDs. However, both scenarios have problems and the existence of this gap remains unexplained (see Bergeron et al. 2001 for a thorough discussion of this problem). Overall, these findings reveal a complex spectral evolution for cool WDs.

Recent advances in the modeling of cool WD atmospheres have raised questions about this complex evolutionary picture. Inclusion of the Lyα far red wing opacity (Kowalski & Saumon 2006) as well as nonideal physics of dense helium that includes refraction (Kowalski & Saumon 2004), ionization equilibrium (Kowalski et al. 2007), and the nonideal dissociation equilibrium of H$_2$ (Kowalski 2006a) significantly changes the expected flux distribution for cool WDs. With their new models, Kowalski & Saumon (2006) demonstrated that cool WD SEDs can be reliably fit with the models including the Lyα opacity. A recent analysis of the Bergeron et al. (2001, 2005) data sets suggests that WDs cooler than 6000 K have either pure H or mixed H/He atmospheres with He/H < 10 (Kowalski 2006b; Kowalski & Saumon 2006). This statement is an important outcome of the new WD atmosphere models that are quite successful so far, but the models need to be tested with further near-infrared observations.

We have undertaken a large near-infrared photometric and spectroscopic survey of the cool WDs discovered by Kilic et al. (2006c) and Harris et al. (2006) in order to perform a detailed model atmosphere analysis of these stars. The choice of H or He composition affects the luminosities for stars with $M_{bol} > 14$. We have selected all WDs with $M_{bol} > 14$ from the Harris et al. (2006) luminosity function for follow-up near-infrared

Table 1
Cool White Dwarfs with IRTF Photometry

SDSS J	u (mag)	g (mag)	r (mag)	i (mag)	z (mag)	J (mag)	H (mag)	K (mag)
02:56:41.61−07:00:33.7	20.757	19.003	18.143	17.793	17.694	16.712 ± 0.046	16.618 ± 0.047	16.484 ± 0.057
03:07:13.90−07:15:06.1	18.632	17.624	17.168	16.980	16.981	16.195 ± 0.044	15.951 ± 0.042	15.874 ± 0.051
03:09:24.87+00:25:25.3	19.119	18.168	17.714	17.523	17.493	16.636 ± 0.033	16.541 ± 0.034	16.869 ± 0.043
04:06:47.32−06:44:36.8	18.844	18.032	17.597	17.491	17.420	16.587 ± 0.046	16.439 ± 0.038	16.271 ± 0.054
07:53:13.27+42:30:01.5	19.948	18.084	17.193	16.877	16.763	15.690 ± 0.031	15.493 ± 0.032	15.470 ± 0.034
11:58:14.51+00:04:58.2	20.871	18.901	17.852	17.529	17.329	16.364 ± 0.034	16.307 ± 0.045	16.185 ± 0.047
13:13:13.12+02:26:45.8	20.980	18.940	17.849	17.477	17.288	16.254 ± 0.033	16.224 ± 0.037	16.129 ± 0.055
13:22:54.60−00:50:42.8	20.668	18.924	18.134	17.821	17.732	16.806 ± 0.047	16.624 ± 0.077	...
14:36:42.78+43:32:35.7	19.823	18.021	17.178	16.844	16.728	15.775 ± 0.035	15.620 ± 0.038	15.510 ± 0.043
15:34:51.02+46:49:49.5	20.892	18.773	17.747	17.366	17.202	16.175 ± 0.032	16.116 ± 0.039	16.037 ± 0.045
17:04:47.69+36:08:47.4	20.512	18.730	17.952	17.663	17.550	16.617 ± 0.034	16.336 ± 0.039	16.324 ± 0.056
21:16:40.30−07:24:52.7	20.261	18.445	17.610	17.283	17.173	16.157 ± 0.037	16.019 ± 0.049	15.898 ± 0.051
22:54:08.63+13:23:57.1	21.592	19.524	18.504	18.157	18.032	17.053 ± 0.024	16.893 ± 0.027	16.875 ± 0.037
23:25:19.88+14:03:39.7	18.040	16.474	15.856	15.574	15.470	14.532 ± 0.041	14.335 ± 0.031	14.207 ± 0.047
23:42:45.75−10:01:21.3	20.466	18.946	18.201	17.936	17.894	17.075 ± 0.060	16.898 ± 0.057	16.792 ± 0.066

Note. The SDSS and IRTF magnitudes are on the AB and MKO system, respectively.

photometric observations at the Infrared Telescope Facility (IRTF) and Gemini. As a backup program, we have obtained near-infrared spectroscopy of relatively brighter targets under non-photometric conditions. Here we present our spectroscopic observations of 38 cool WDs. In addition, we present photometric observations of 15 of these stars. This data set enables us to test the predictions of the model atmospheres and to improve our understanding of the spectral evolution of cool WDs in general. Section 2 describes our observations and fitting procedures, while an analysis of these data and results from this analysis are discussed in Section 3.

2. OBSERVATIONS AND THE FITTING PROCEDURES

We used the 0.8–5.4 μm medium-resolution spectrograph and imager (SpeX; Rayner et al. 2003) on the IRTF to perform near-infrared spectroscopy on 38 cool WDs. The prism mode was employed with a 0″.5 slit to produce spectra with an average resolving power of 150 over the 0.8–2.5 μm range. Our observations were performed under conditions of thin cirrus and partly cloudy skies on several nights in 2004 December, 2005 May, 2005 November, and 2006 April. We aligned the slit along the parallactic angle to minimize slit light losses due to atmospheric refraction. To remove the dark current and the sky signal from the data, the observations were taken at two different positions on the slit separated by 10″. Internal calibration lamps were used for flat-fielding and wavelength calibration, respectively. In order to correct for telluric features and to flux calibrate the spectra, nearby bright A0V stars were observed at an airmass similar to the target star observations. The telluric correction is usually not perfect; the absorption features seen in the spectra of some of our targets in the range 1.3–1.5 μm and 1.8–2.0 μm are due to this problem. We used an IDL-based package, Spextool version 3.4 (Cushing et al. 2004), to reduce our data.

Under photometric conditions, we used the Spex guide camera to obtain *JHK* photometry of 15 of the WDs from our spectroscopy sample. A five- or nine-position dither pattern with 60 s exposures was used. UKIRT faint standards were used to calibrate the photometry. The derived magnitudes in the Mauna Kea photometric system are presented in Table 1. The rest of the WDs in our spectroscopy sample are presented in Table 2. Ten of
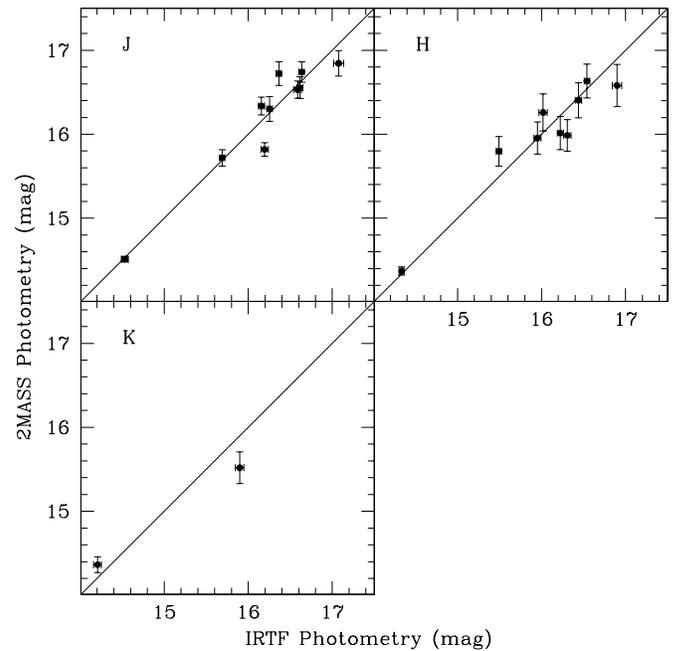
Figure 1. IRTF photometry of our targets compared to the 2MASS photometry.

these stars are also detected in the Two Micron All Sky Survey (2MASS), at least in the *J* band. Figure 1 shows a comparison between the IRTF and 2MASS photometry. Our photometry is consistent with the lower quality 2MASS data within the errors.

Optical spectroscopy of the majority of our targets was presented in Kilic et al. (2006c). Four targets have spectroscopy available in the literature. We have obtained optical spectroscopy of the remaining six WDs using the Hobby–Eberly Telescope (HET) equipped with the Marcario Low-Resolution Spectrograph. Our observations were performed in the queue mode between UT 2005 January 8 and 2006 January 6. Grism 2 with a 1″.5 slit produced spectra with a resolution of 6 Å over the range 4280–7340 Å. Figure 2 presents the optical spectra of the six new WDs observed at the HET. One of these objects, J1237+4156 (LHS 5222, also in Kawka & Vennes 2006), is a DQ WD with strong C_2 Swan bands. Another object, J1424+6246, displays Hα and is therefore classified DA. The remaining four WDs

Table 2
Cool White Dwarfs with IRTF Spectroscopy

SDSS J	u (mag)	g (mag)	r (mag)	i (mag)	z (mag)	$J-H$ (mag)	$H-K_s$ (mag)
00:11:42.66−09:03:24.3	18.541	17.880	17.530	17.397	17.385	0.21	−0.16
01:21:44.78+00:11:43.2	19.298	18.233	17.724	17.582	17.532	0.41	0.10
01:28:27.47−00:45:12.5	18.880	17.853	17.456	17.301	17.295	0.22	0.14
07:48:11.90+35:06:32.3	19.469	18.300	17.880	17.769	17.812	0.30	0.24
08:17:51.52+28:22:03.1	21.601	19.498	18.622	18.310	18.246	0.29	0.09
10:48:01.84+63:34:48.8	19.336	17.931	17.308	17.031	17.019	0.28	0.06
11:15:36.95+00:33:17.3	19.462	17.922	17.215	16.960	16.896	0.30	0.09
12:03:28.64+04:26:53.4	19.530	18.177	17.502	17.222	17.152	0.06	−0.28
12:37:52.12+41:56:25.8	17.822	17.789	17.128	16.857	16.979	0.13	0.05
13:33:59.85+00:16:54.7	19.020	19.409	18.323	18.078	18.173	0.43	−0.05
13:45:32.91+42:00:44.1	19.707	17.879	17.014	16.728	16.588	0.27	0.07
14:24:29.51+62:46:17.0	20.327	18.828	18.144	17.896	17.730	0.26	0.12
14:40:18.80+13:18:35.3	20.079	18.862	18.293	18.062	17.996	0.39	0.13
14:52:24.95−00:11:34.7	19.839	18.444	17.816	17.598	17.504	0.32	0.03
15:48:35.88+57:08:26.4	18.520	17.749	17.340	17.216	17.172	0.17	−0.02
16:07:14.18+34:23:45.7	18.538	17.476	16.948	16.779	16.756	0.28	0.02
16:54:45.69+38:29:36.5	17.930	16.994	16.577	16.425	16.412	0.24	0.01
21:47:52.09−08:24:36.7	18.546	17.769	17.403	17.242	17.237	0.20	0.02
21:54:30.69+13:00:26.7	20.674	19.057	18.361	18.071	17.943	0.24	0.02
22:22:33.90+12:21:42.9	21.450	19.435	18.334	17.932	17.724	0.12	−0.03
22:41:57.62+13:32:38.8	18.399	17.547	17.147	17.032	16.996	0.14	0.00
23:12:06.08+13:10:57.6	19.169	17.732	17.091	16.895	16.787	0.24	0.08
23:37:07.67+00:32:42.2	19.282	18.262	17.783	17.625	17.640	0.33	0.02

Note. The near-infrared colors are calculated using our IRTF spectra and they are given in the 2MASS system.
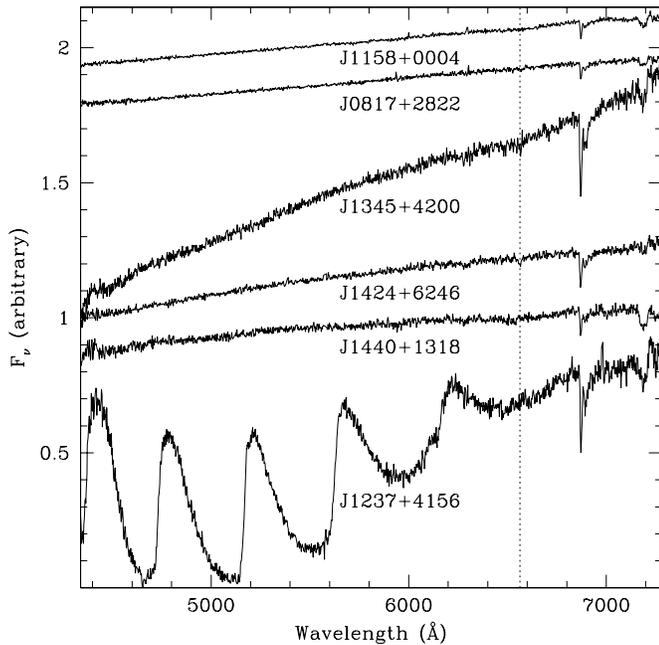
Figure 2. Optical spectra for the new WDs observed at the HET. The dotted line marks Hα, which is detected only for J1424+6246. The spectral features present in all of our spectra at 6890 Å and 7200 Å are telluric. The $g - i$ color increases from bottom to top, with the exception of J1237+4156.

show featureless spectra. The spectral types for all of our targets are presented in Table 3, which also includes the telescopes that were used to obtain the spectra. The 2.7 m telescope spectra do not cover Hα, and we cannot rule out the DA classification for these stars.

We use pure H, pure He, and mixed H/He atmosphere models with $\log g = 8$ to fit the optical and near-infrared photometry of our targets. We use the zero points derived from the Space Telescope Imaging Spectrograph (STIS) spectrum of Vega (Bohlin & Gilliland 2004) integrated over the passband for each filter. The resulting fluxes are then compared with those predicted from the model atmospheres, integrated over the same bandpass.

3. RESULTS

3.1. WDs with Near-Infrared Photometry

We have *JHK* photometry for less than half of our sample. We use these stars to demonstrate that our near-infrared spectroscopy is indeed accurate enough for studying the SEDs of cool WDs.

Figures 3 and 4 show the optical and near-infrared photometry and IRTF spectroscopy of 11 DC and three DA WDs. The IRTF spectra are normalized to match the *zJHK* photometry. The mean differences between synthetic photometry derived using the IRTF spectra and the observed photometry for the 14 stars presented in these figures are 1% ± 4% in *z*, 5% ± 4% in *J*, 1% ± 6% in *H*, and 2% ± 8% in *K*. Thus, the absolute flux calibration of our spectra is accurate to 5%–10%.

Best-fit pure H, pure He, and mixed H/He models are shown as solid, dotted, and dashed lines, respectively. The parameters for the best-fit models are given in each panel. The spectra of none of these WDs are consistent with pure He models of any temperature as they do not resemble blackbodies. The pure H and mixed H/He models by Kowalski & Saumon (2006) reproduce the observed SEDs fairly well for these stars. Even though one cannot differentiate between H and He atmosphere models based on the optical data only, our IRTF photometry and spectroscopy data show that these stars have hydrogen-rich composition. We confirm that the models including the Lyα opacity are reliable and they reproduce the entire SEDs of WDs as cool as 4250 K.

Table 3
Atmospheric Parameters of Cool White Dwarfs

Object	SpType	He/H	T_{eff} (K)	Optical Spectrum	Reference
J0011−0903	DA	0	6290	2.7 m	K06
J0121+0011	...	...	5530	...	...
J0128−0045	DA	0	5760	2.7 m	K06
J0256−0700	DC	0.4	4660	MMT	K06
J0307−0715	DA	0	5730	CTIO	O01
J0309+0025	DC	17.5	5600	2.7 m	K06
J0406−0644	DA	0	5910	2.7 m	K06
J0748+3506	DZA	2.3	5700	2.7 m	K06
J0753+4230	DC	0	4570	2.7 m	K06
J0817+2822	DC	0	4550	HET	TS
J1048+6334	DA	0	5170	MMT	K06
J1115+0033	DA	0	5010	MMT	K06
J1158+0004	DC	0	4350	HET	TS
J1203+0426	DC	8.5	5040	MMT	K06
J1237+4156	DQ	He	6000:	HET	TS
J1313+0226	DC	0	4250	MMT	K06
J1322−0050	DC	0.7	4760	MMT	K06
J1333+0016	DQ	He	5220:	SDSS	...
J1345+4200	DC:	0	4640	HET	TS
J1424+6246	DA	0	5010	HET	TS
J1436+4332	DC	0.3	4670	...	H86
J1440+1318	DC	0	5340	HET	TS
J1452−0011	DC	0	5200	2.7 m	K06
J1534+4649	DC	0	4280	...	H86
J1548+5708	DC	He	5810	2.7 m	K06
J1607+3423	...	...	5600	...	...
J1654+3829	DZA	6.2	5830	2.7 m	K06
J1704+3608	DC	0.4	4770	HET	K06
J2116−0724	DC	0	4660	2.7 m	K06
J2147−0824	DA	0	6110	2.7 m	K06
J2154+1300	DZA	1.1	4930	MMT	K06
J2222+1221	DC	0	4170	HET	K06
J2241+1332	DA	0	6000	2.7 m	K06
J2254+1323	DC	0	4340	HET	K06
J2312+1310	DA:	0	5240	2.7 m	K06
J2325+1403	DC	0.6	5040	2.7 m	K06
J2337+0032	DA	0	5800	2.7 m	K06
J2342−1001	DA	0	5070	MMT	K06

Note. The references are as follows: H86, Hintzen (1986); K06, Kilic et al. (2006c); O01, Oppenheimer et al. (2001); TS, this study.

The near-infrared photometry and spectroscopy of some of these stars show small deviations from the pure H models. We classify these stars as mixed H/He atmosphere WDs that are affected by the additional opacity from H_2–He CIA. Since He atmospheres are much denser than the H atmospheres at the same temperature, the CIA opacity is stronger in mixed atmospheres compared to pure H atmospheres. Given the observational errors, one can argue that it is not always straightforward to choose between the pure H and mixed H/He models. However, this does not affect our main conclusion that these WDs do not have pure He atmospheres, and they have hydrogen-dominated atmospheres with He/H $\leqslant$ 1.

We note that the SEDs of the DC WDs with $T_{eff} >$ 4500 K can also be explained with the Bergeron et al. (1995) pure He models. Kowalski (2006b) proposed to solve this ambiguity by calculating new pure He models, which include improved physics for dense helium, and a better calculation of the ionization equilibrium, the He$^-$ free–free (Kowalski et al. 2007), and Rayleigh scattering absorptions (Iglesias et al. 2002). These new models predict a higher
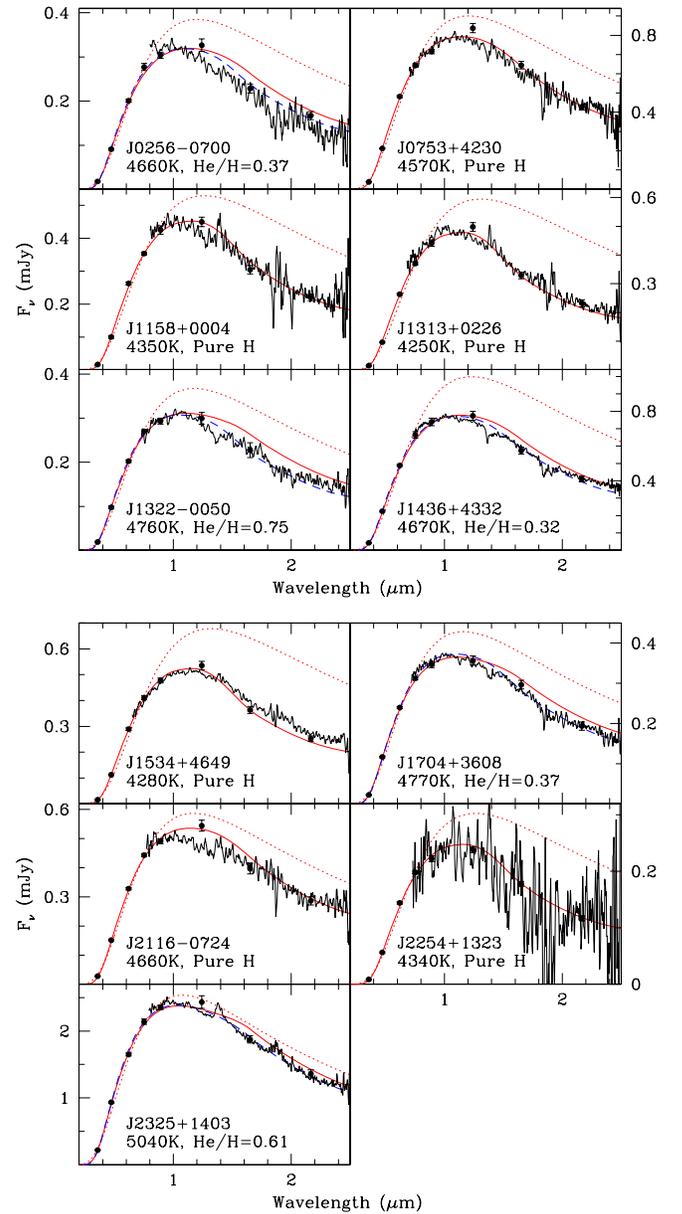
Figure 3. SEDs of DC WDs with IRTF photometry and spectroscopy compared to best-fit pure H (solid lines), pure He (dotted lines), and mixed H/He (dashed lines) atmosphere models.
(A color version of this figure is available in the online journal.)

ionization fraction and He$^-$ free–free opacity and a smaller contribution from Rayleigh scattering opacity. The colors for the Kowalski (2006b) pure He sequence are quite different than the Bergeron et al. (1995) pure He sequence; they are close to those of blackbodies and therefore they predict more flux in the B band and less flux around 1 μm (see Figure 13 of Bergeron et al. 1995). For example, Bergeron et al. (1995) pure He models with $\log g = 8$ predict $g-i$ colors of 0.5, 1.1, and 2.1 mag for WDs with $T_{eff} = 6000$, 5000, and 4000 K, respectively. On the other hand, Kowalski (2006b) models predict $g - i \approx 0.5$, 0.9, and 1.4 mag for the same gravity and temperature models, respectively.

3.2. WDs with Near-Infrared Spectroscopy

For the stars with only near-infrared spectroscopy data, we performed synthetic photometry on the IRTF spectra using the
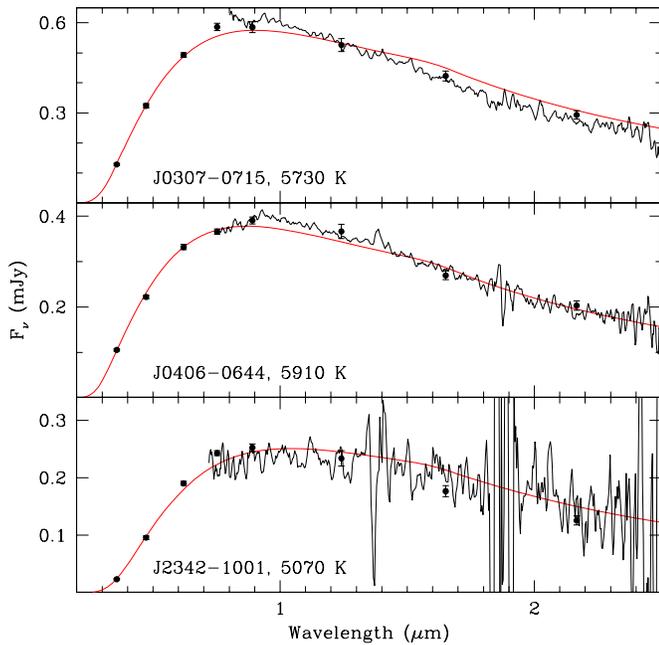
Figure 4. SEDs of DA WDs with IRTF photometry and spectroscopy compared to pure H atmosphere models.

(A color version of this figure is available in the online journal.)

Figure 5. SEDs of DC WDs with IRTF spectroscopy compared to best-fit pure H (solid lines) and pure He (dotted lines) models.

(A color version of this figure is available in the online journal.)

2MASS filter transmission curves. Since the IRTF spectra are reliable down to 0.8 μm, we normalize the spectra to match the SDSS z-band photometry. This normalization should result in near-infrared fluxes that are accurate to 5%–10%. A comparison between our synthetic photometry and 2MASS photometry shows an overall agreement within the errors. Due to large errors in 2MASS photometry for these faint targets, we do not use it in our fits, but we show it in all figures for comparison.

3.2.1. DC WDs

We use pure H and pure He atmosphere models to fit the SDSS photometry and IRTF synthetic photometry of our targets. Given the 5%–10% errors in the absolute flux calibration of our spectra, we do not perform fits using mixed H/He models for these stars. Figure 5 presents the SEDs of six DC WDs with near-infrared spectroscopy. The observed spectra are in good agreement with predictions from the model atmosphere calculations. For example, the entire SED of J2222+1221 is fit extremely well by a pure H atmosphere model with $T_{\rm eff} = 4170$ K. Three of the stars in this figure are warmer than 5000 K. Hα should be visible for these WDs if they have pure H atmospheres. A comparison of the observed optical and infrared SEDs with model predictions shows that J1548+5708 is the only pure He atmosphere WD in this sample. Even though the difference between the pure H and pure He atmosphere models is less significant in the infrared at these temperatures, J1548+5708 does not show any hydrogen lines in its optical spectrum, and the observed SED is best explained with a 5810 K pure He atmosphere model. J1440+1318 and J1452−0011 seem to fit pure H models best, but their infrared spectra are noisy and their identification as pure H atmosphere WDs remains questionable. In addition, the optical spectrum of J1452−0011 was obtained at the McDonald 2.7 m telescope. Hence, a DA classification is possible for this star.
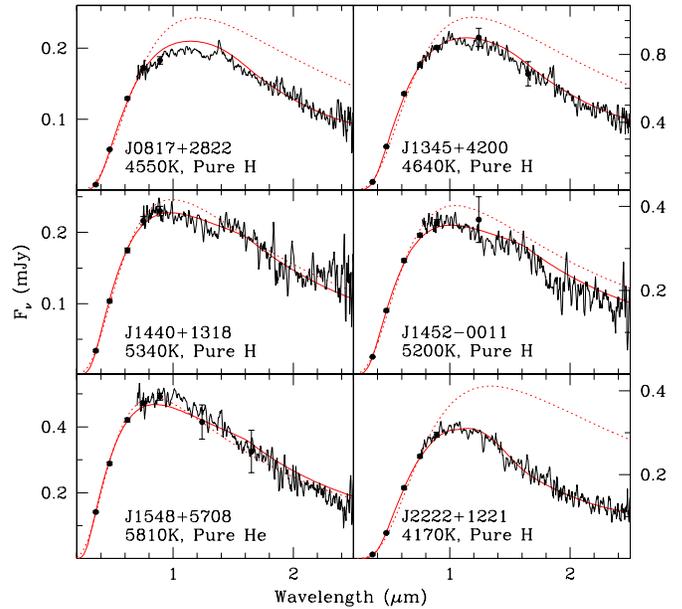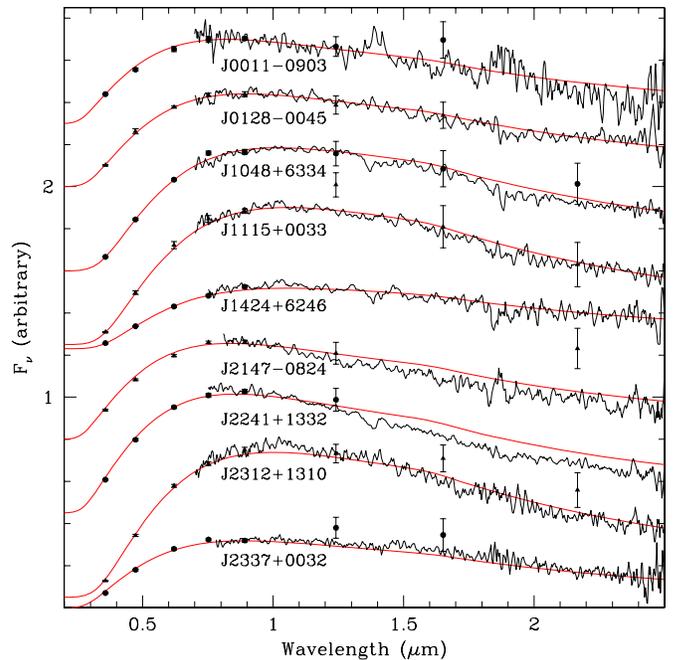
Figure 6. SEDs of DA WDs with IRTF spectroscopy compared to pure H atmosphere models.

(A color version of this figure is available in the online journal.)

3.2.2. DA WDs

It is easier to classify the WDs hotter than 5000 K based on their optical spectroscopy as they are expected to show Hα if they have hydrogen-rich atmospheres. Figure 6 presents the SEDs for nine DA WDs. Bergeron et al. (2001) found that the pure H models are in good agreement with Hα spectroscopy of most stars in their sample. Thus, we adopt the pure H atmosphere solutions for all these DAs. Like the DAs presented in Figure 4, the SEDs are explained fairly well by pure H models with $T_{\rm eff} = 5000$–6300 K.
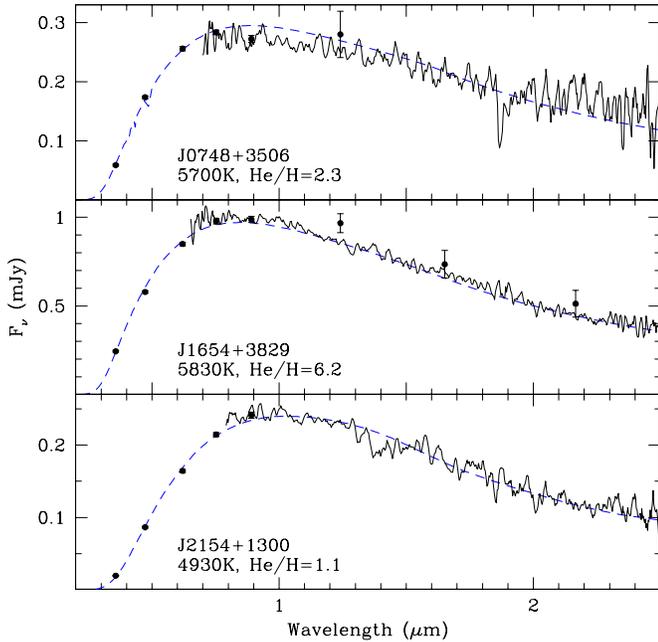
Figure 7. SEDs of DZA WDs compared to best-fit mixed H/He (dashed lines) atmosphere models.

(A color version of this figure is available in the online journal.)

3.2.3. DZA WDs

Three of the stars in our sample show metal and hydrogen lines in their optical spectra, and they are classified DZA. They should have helium-dominated atmospheres contaminated with metals and hydrogen. Figure 7 displays the optical and near-infrared SEDs for these three stars compared to mixed H/He atmosphere model predictions. As expected, they are best explained with mixed H/He atmosphere models with He/H ratios greater than 1. Given the errors in absolute flux calibration of our spectra, these He/H ratios should be used with caution. A detailed analysis using optical spectroscopy is required to accurately determine their metal and hydrogen abundances.

3.2.4. DQ WDs

There are two DQ WDs, J1237+4156 and J1333+0016, in our sample, and we mention them for completeness purposes, but we do not present our near-infrared spectroscopy of these objects in this paper. These stars need to be modeled with proper model atmospheres including carbon. Such an analysis shows that J1237+4156 has $T_{eff} \approx 6000$ K and J1333+0016 has $T_{eff} < 6000$ K (P. Dufour 2008, private communication). In addition, optical spectroscopy is not available for one of our targets, J1607+3423. We do not show the IRTF spectrum of this target, but its SED is best explained as a 5600 K WD.

3.3. WDs with Strong Flux Deficits

Figure 8 displays an optical–infrared color–color diagram for our sample. Stars with IRTF photometry are shown as filled dots with error bars. Six cool WDs studied by Bergeron et al. (2001) are covered by the SDSS imaging and included here for comparison. In addition, we transformed the *BVRI* photometry of LHS 1126, a peculiar WD with strong infrared flux deficits (Wickramasinghe et al. 1982; Kilic et al. 2006b, 2008), to the SDSS filter system using the transformations given in Smith
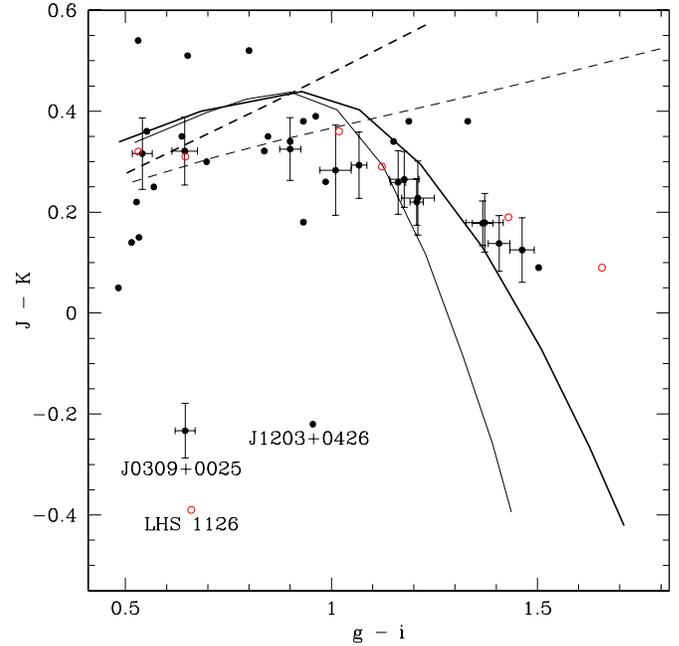
Figure 8. Optical–infrared color–color diagram for our sample of WDs with and without IRTF photometry (filled dots with and without error bars, respectively). Six WDs with *JHK* photometry from Bergeron et al. (2001; open circles) are also detected in the SDSS and plotted here for comparison. The transformed colors of LHS 1126, a peculiar WD with a strong near-infrared flux deficit, are also shown. Thick (thin) solid and dashed lines show the cooling sequences for the Kowalski (Bergeron et al. 2001) pure H (6000–3500 K) and pure He atmosphere models (6000–4250K) with log $g = 8$, respectively.

(A color version of this figure is available in the online journal.)

et al. (2002).[5] The $g - i$ and $J - K$ colors for our sample of WDs are consistent with the six WDs studied by Bergeron et al. (2001). The thick solid and dashed lines show the pure H and pure He models by Kowalski (2006b), respectively. The thin lines show similar models by Bergeron et al. (1995). The only significant difference between the pure H models by Kowalski & Saumon (2006) and Bergeron et al. (1995) is the inclusion of the Lyα opacity, which suppresses the g-band flux and makes the model $g - i$ colors redder. Compared to the pure H models, the differences between the pure He models are more significant. The coolest WDs in our sample ($g - i > 1.3$ mag) do not follow either of the pure He model atmosphere sequences. There are two stars, J0309+0025 and J1203+0426, with colors similar to LHS 1126 and with strong near-infrared flux deficits. Both of these stars have featureless optical spectra (DC spectral type; Kilic et al. 2006c).

The top panel in Figure 9 shows the J0309+0025 SED compared to pure H and mixed atmosphere models. Our IRTF photometry also confirms the flux suppression observed in the spectrum. Even though the mixed H/He model is not a perfect fit to the observed SED, it is definitely better than the pure H or pure He atmosphere solutions. Therefore, J0309+0025 is best explained as a mixed atmosphere WD with a He/H ratio of 17.5. The J1203+0426 SED is shown in the bottom panel. Our IRTF spectrum favors a mixed atmosphere solution with He/H = 8.5, and the overall flux distribution is reproduced fairly well by

---

[5] The optical spectrum of LHS 1126 shows an absorption feature centered at 5000 Å. This feature is 15% deep at the center compared to the continuum flux (see Figure 3 in Bergeron et al. 1994), and it affects the color transformations slightly. However, we use the transformed $g - i$ color for illustration purposes only.
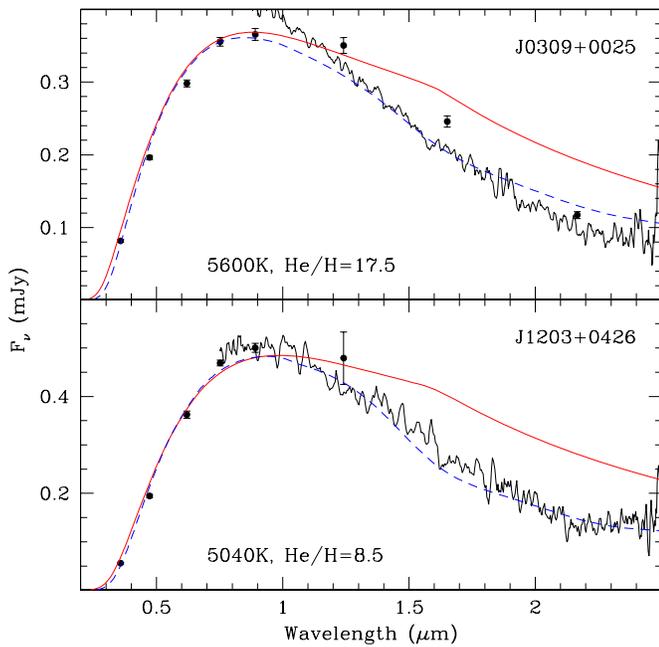
Figure 9. SEDs of two stars with strong near-infrared flux deficits along with best-fit pure H (solid lines) and mixed H/He (dashed lines) atmosphere models.

(A color version of this figure is available in the online journal.)

Figure 10. SED of a star that shows near-infrared flux excess. The bottom panel shows the excess flux after subtracting the expected flux from the WD. The red solid line in the bottom panel shows the expected flux distribution for an M5V star.

(A color version of this figure is available in the online journal.)

this model. This figure demonstrates that both J0309+0025 and J1203+0426 are best explained with mixed H/He atmosphere models.

3.4. Stars with Infrared Excess

There is only one object in our sample that shows a significant flux excess in the near-infrared. Figure 10 shows the SED of J0121+0011, and the excess flux observed. Both 2MASS photometry and our IRTF spectroscopy of J0121+0011 show excess flux longward of 1.1 μm, though the 2MASS photometry is also consistent with no excess. Optical spectroscopy is not available for this star, however its optical colors are consistent with pure H atmosphere models. Normalizing the IRTF spectrum to the 2MASS photometry in the J band, the observed excess is $\approx$0.03, 0.06, and 0.04 mJy in the J, H, and K band, respectively. If the excess is caused by a binary companion, this corresponds to $M_K = 14.7$ mag, a T dwarf (Leggett et al. 2002). However, the observed infrared excess is not compatible with a T dwarf companion. The bottom panel in this figure shows the flux distribution for an M5V star (Pickles 1998), which is roughly consistent with the observed excess. However, a late-type M dwarf would have $M_K < 10$ mag for M8V or earlier spectral-type stars. Hence, if this excess is real, it can only come from a background object.

4. DISCUSSION

Understanding the spectral evolution of WDs is critical for assigning ages to cool WDs. Without knowing the previous history of each WD, we can only use large samples of WDs to statistically decide how much time they spend as helium versus hydrogen atmosphere objects and therefore deduce their ages.

Cool WDs with hydrogen atmospheres are expected to turn into helium-rich atmospheres if the superficial hydrogen layer becomes convective over a significant fraction of its depth. If the hydrogen envelope is thin enough, the bottom of the hydrogen convection zone can reach the underlying more massive helium layer resulting in convective mixing. The effective temperature at which this mixing occurs depends on the thickness of the envelope. Stars with thicker envelopes are expected to mix at lower temperatures, and stars with $M_H \sim 10^{-6} M_\star$ are not expected to mix at all (see the discussion in Tremblay & Bergeron 2008).
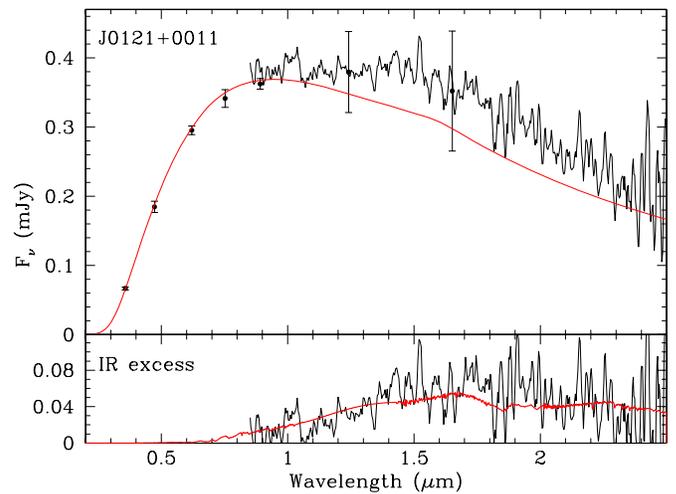
Studying the 2MASS photometry of spectroscopically confirmed WDs, Tremblay & Bergeron (2008) found that the ratio of helium to hydrogen atmosphere WDs gradually increases from 25% for 10000–15000 K to 45% for 5000–9000 K. They explain this increase as a result of convective mixing for about 15% of the DAs that have hydrogen envelope masses in the range 10^{-10} to 10^{-8} $M_\star$. They do not find any evidence for convective mixing below 8000 K, which implies a discontinuity in the hydrogen layer mass distribution, with the majority of the DAs having hydrogen layers more massive than 10^{-6} $M_\star$.

The spectral evolution of cooler WDs was studied by Bergeron et al. (2001), who found a non-DA gap in the temperature range 5000–6000 K. The existence of this gap depends on the re-appearance of non-DAs below 5000 K, which of course depends on their correct classification. Based on the recent model atmosphere calculations presented by Kowalski & Saumon (2006), we have shown that the majority of the stars in our sample have hydrogen-rich atmospheres. This is true for both our near-infrared photometry and spectroscopy samples. The exceptions are the two DQ WDs with helium-dominated atmospheres and J1548+5708 with a pure He atmosphere. All of these stars are warmer than 5000 K. We do not find any pure He atmosphere stars below 5000 K. Therefore, the 5000–6000 K non-DA gap seems to be dependent on which models are applied to WDs cooler than 5000 K.

Considering the work of Kowalski & Saumon (2006), which has demonstrated that the optical and near-infrared SEDs of cool WDs are explained fairly well with the new pure hydrogen models, this result is not surprising. Based on these models, almost all cool WDs have hydrogen-rich composition, and all of them turn into pure hydrogen atmosphere objects below about 4500 K (see Kowalski 2006b). Therefore, instead of a complex spectral evolution scenario, these results suggest a simpler scenario in which the hydrogen abundance increases with time. Kowalski (2006b) argued that accretion could be responsible

for the observed trend in hydrogen enrichment. Assuming that the accreted gas has a composition H/He $\sim$ 10, he found that a constant accretion rate of $\dot{M} = 6 \times 10^{-17}$ $M_\odot$ yr^{-1} could explain the observations.

An important test for the hydrogen accretion scenario is whether the accretion rate is compatible with the observations of warmer WDs or not. A detailed model atmosphere analysis of a large sample of metal-rich helium atmosphere (DZ) WDs by Dufour et al. (2007) found that the hydrogen abundances in DZs with $T_{\rm eff} = 6000$–12000 K are consistent with accretion rates of 10^{-20} to 10^{-18} $M_\odot$ yr^{-1}. This is at least 2 orders of magnitude smaller than the accretion rate found by Kowalski (2006b). The systematic differences between the different models used in the analyses could be responsible for the discrepancy in the hydrogen accretion rates. Further testing is required to check if the Kowalski (2006b) models imply significant differences in hydrogen abundances for DZs.

The high hydrogen accretion rate would suggest that DQ, as well as DC and DZ, WDs should turn into mixed atmosphere stars below 6000 K. Dufour et al. (2005) demonstrated that the number of DQs shows a drop at about $T_{\rm eff} \approx 7000$ K and an abrupt cutoff at 6000 K. Out of the 56 stars in their sample, they found only one DQ cooler than 6000 K, which is predicted to be a massive WD. Dufour et al. concluded that the physical mechanism for this cutoff is unknown, but it may be related to the existence of the peculiar DQ stars at lower temperatures (also see Bergeron et al. 1997). Perhaps it is noteworthy to mention that G99−37, the only DQ that shows hydrogen absorption, is right at the boundary with $T_{\rm eff} = 6070$ K. If the DQp stars have mixed C/He/H atmospheres, the hydrogen accretion scenario could explain the disappearance of DQs below 6000 K and the emergence of the DQp stars. Even though the shifted Swan bands in peculiar DQs were originally thought to originate from the C$_2$H molecule (Schmidt et al. 1995), Hall & Maxwell (2008) now argue that the observed bands are not compatible with C$_2$H absorption and they are most likely pressure-shifted Swan bands. Therefore, there is no conclusive evidence of hydrogen accretion in cool DQs.

5. CONCLUSIONS

Based on the recent model atmosphere calculations presented by Kowalski (2006b), our analysis of the optical and near-infrared SEDs of several dozen cool WDs showed that the majority of the WDs with $T_{\rm eff} \leqslant 6000$ K have hydrogen-rich atmospheres. There are a few WDs warmer than 5000 K that (may) possess pure He atmospheres, but we do not find any non-DAs cooler than 5000 K. Therefore, the existence of the non-DA gap between 5000 K and 6000 K seems to depend on the models used in the analysis.

We find two WDs with significant flux deficits and their SEDs are best explained with mixed H/He atmosphere models. Even though convective mixing is believed to dominate the spectral evolution of WDs with $T_{\rm eff} \approx 15000$–6000 K, the ISM accretion may dominate at cooler temperatures and explain the observed trend in helium to hydrogen ratios by converting helium atmosphere objects into hydrogen-dominated atmospheres. However, the required hydrogen accretion rate is 2 orders of magnitude

higher than the rate derived from the analysis of warmer WDs. Hence, our understanding of the spectral evolution of WDs remains incomplete.

REFERENCES

Bergeron, P., Leggett, S. K., & Ruiz, M. T. 2001, ApJS, 133, 413
Bergeron, P., Ruiz, M. T., Hamuy, M., Leggett, S. K., Currie, M. J., Lajoie, C.-P., & Dufour, P. 2005, ApJ, 625, 838
Bergeron, P., Ruiz, M. T., & Leggett, S. K. 1997, ApJS, 108, 339
Bergeron, P., Saumon, D., & Wesemael, F. 1995, ApJ, 443, 764
Bergeron, P., et al. 1994, ApJ, 423, 456
Bohlin, R. C., & Gilliland, R. L. 2004, AJ, 127, 3508
Cushing, M. C., Vacca, W. D., & Rayner, J. T. 2004, PASP, 116, 362
Dufour, P., Bergeron, P., & Fontaine, G. 2005, ApJ, 627, 404
Dufour, P., et al. 2007, ApJ, 663, 1291
Eisenstein, D. J., et al. 2006, ApJS, 167, 40
Gates, E., et al. 2004, ApJ, 612, 129
Hall, P. B., & Maxwell, A. J. 2008, ApJ, 678, 1292
Hansen, B. M. S. 1998, Nature, 394, 860
Hansen, B. M. S. 1999, ApJ, 520, 680
Hansen, B. M. S., et al. 2007, ApJ, 671, 380
Harris, H. C., et al. 2006, AJ, 131, 571
Harris, H. C., et al. 2008, ApJ, 679, 697
Hintzen, P. 1986, AJ, 92, 431
Iglesias, C. A., Rogers, F. J., & Saumon, D. 2002, ApJ, 569, L111
Kawka, A., & Vennes, S. 2006, ApJ, 643, 402
Kilic, M., Kowalski, P. M., Mullally, F., Reach, W. T., & von Hippel, T. 2008, ApJ, 678, 1298
Kilic, M., von Hippel, T., Leggett, S. K., & Winget, D. E. 2006a, ApJ, 646, 474
Kilic, M., von Hippel, T., Mullally, F., Reach, W. T., Kuchner, M. J., Winget, D. E., & Burrows, A. 2006b, ApJ, 642, 1051
Kilic, M., et al. 2006c, AJ, 131, 582
Koester, D., & Wolff, B. 2000, A&A, 357, 587
Kowalski, P. M. 2006a, ApJ, 641, 488
Kowalski, P. M. 2006b, PhD thesis, Vanderbilt Univ.
Kowalski, P. M., & Saumon, D. 2004, ApJ, 607, 970
Kowalski, P. M., & Saumon, D. 2006, ApJ, 651, L137
Kowalski, P., et al. 2007, Phys. Rev. B., 2007, 76
Leggett, S. K., et al. 2002, ApJ, 564, 452
Munn, J. A., et al. 2004, AJ, 127, 3034
Oppenheimer, B. R., Hambly, N. C., Digby, A. P., Hodgkin, S. T., & Saumon, D. 2001, Science, 292, 698
Pickles, A. J. 1998, PASP, 110, 863
Rayner, J. T., Toomey, D. W., Onaka, P. M., Denault, A. J., Stahlberger, W. E., Vacca, W. D., Cushing, M. C., & Wang, S. 2003, PASP, 115, 362
Saumon, D., & Jacobson, S. B. 1999, ApJ, 511, 107
Schmidt, G. D., Bergeron, P., & Fegley, B., Jr. 1995, ApJ, 443, 274
Smith, J. A., et al. 2002, AJ, 123, 2121
Tremblay, P. E., & Bergeron, P. 2008, ApJ, 672, 1144
Wickramasinghe, D. T., Allen, D. A., & Bessel, M. S. 1982, MNRAS, 198, 473